CURVATURE EFFECTS ON POST-TENSIONED CONCRETE BOX GIRDER BRIDGES WITH EXTERNAL TENDONS

Bo Hu, Ph.D., P.E., PBS&J, Inc., Tampa, FL

Dongzhou Huang, Ph. D., P.E., PBS&J, Inc., Tampa, FL

ABSTRACT

This paper presents the effects of curvature on normal stress, shear stress and bearing reaction of post-tensioned box girder bridges with external tendons subjected to self weight, live load, post-tensioning and combined effects. First, a brief description of the prototypical bridges which were analyzed in the parametric study is given followed by the three-dimensional models. An extensive numerical analysis on the effect of curvature was performed by changing radius from an infinite value to 300-ft. Finally, recommendations for implementation in bridge design are provided. Results show that simplified straight models may not be directly used for proper structural response estimation for post-tensioned curved box girder bridges.

Keywords: Curvature, Box Girder, Bridge, Post-Tensioning, External Tendon

INTRODUCTION

The need for a smooth dissemination of congested traffic, the limitation of right-of-way along with economic, aesthetic and environmental considerations have motivated the increased use of curved box girder bridges. AASHTO LRFD Specifications (2007) allow curvature effects to be neglected in flexural design for curved steel multiple-beam superstructure types with a central span angle less then 12 degrees. Thompson et al. (1998) investigated the effects of curvature on normal stresses due to live load and concluded that the curvature effects can be neglected for segmental concrete box bridges with a central angle up to 15 degrees. However, the majority of proceeding investigations had not studied the effects of curvature on shear and support reaction due to self weight and external post-tensioning. AASHTO Specifications do not provide guidelines for curved segmental concrete bridges regarding this issue.

This paper investigates the effects of curvature in post-tensioned concrete bridges with external tendons, and the post-tensioning design method for accomplishing a reasonable force condition under design loads. First, 3-D finite element models are established for a series of prototype bridges with different curvature radii. The effects due to dead load and post-tensioning are then studied in comparison to the results of straight bridges. Based on the effects of curvature on normal stress, shear stress and the bearing reactions; the criterion for neglecting these effects is discussed. Finally, recommendations are made to the current standard design practice based on the analysis results.

DESCRIPTION OF BRIDGES

The prototypical example used for this analysis is a typical three-span continuous box girder bridge. The radii investigated are: infinite (i.e. straight bridge), 2000 ft, 1000 ft, 650 ft, and 300 ft. All bridge models have the same span layout between supports, 150ft + 200 ft + 150 ft, as shown in Figure 1. Table 1 provides the span angle change of both end spans and center spans for all the considered cases. The same prismatic cross section is adopted for each bridge model as presented in Figure 2. In order to simplify modeling process, the top slab is held at a constant thickness.

Table 1 Span Angle Change of Bridges (in degree)

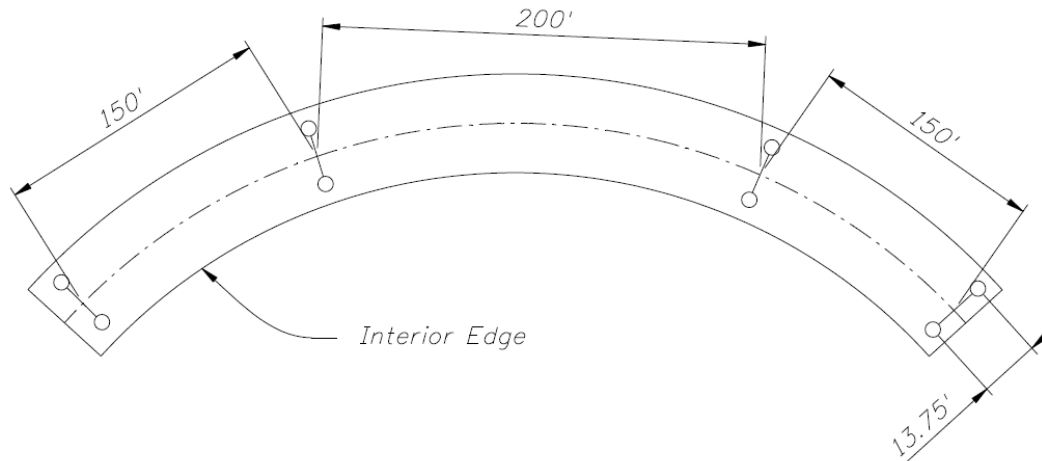| Radius	Infinite	2000 ft	1000 ft	650 ft	300 ft
End Span	0	4.30	8.59	13.22	28.65
Center Span	0	5.73	11.46	17.63	38.20

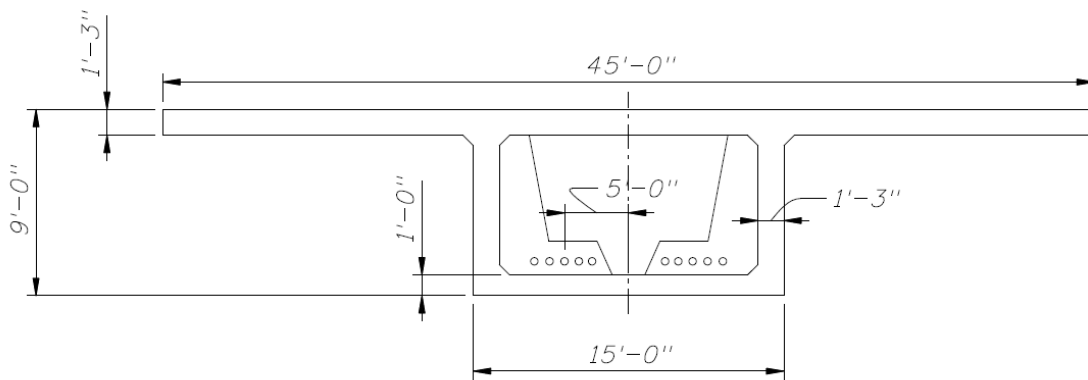Figure 1 Bridge Layout Along the Box Centerline

Figure 2 Box Girder Cross Section

At each pier location, two rigid vertical supports are provided underneath the bottom slab of the box at the center line of the webs. Besides, one transverse constraint and two longitudinal constraints are placed at the beginning of each bridge model for stability. All supports are free to rotate. This boundary condition eliminates rigid body movement, keeps free in-plane elastic deformation and provides rigid torsional restraint at each pier location. Diaphragms with 6 ft thickness are used at all pier locations to limit local effects and anchor the post-tensioning tendons.

All the bridges are post-tensioned using the same amount of external prestressing tendons and the same tendon layout both transversely and longitudinally along the bridge centerlines. 17.577 in^2 (3x27K6) and 29.295 in^2 (5x27K6) of 270 ksi prestressing tendons are used for each web of the end spans and the center span, respectively. The tendon quantity is

determined such that the structure has no tensile stress developed at the critical sections, under the combined effects of dead load and live load (around 45% of positive moment due to dead load). Vertical deviators are placed at quarter span locations for every span. Horizontal deviators are located at mid-span for each of the end spans and 3/8 span locations (3/8L and 5/8L) for the center spans. The vertical eccentricities of the external tendons are 1 ft from the box bottom at deviator locations and 1 ft from the box top at all diaphragm locations. Horizontally, the external tendon centroid is located at an offset of 5 ft from the box center line. Figure 3 shows the details of the post-tensioning layout.
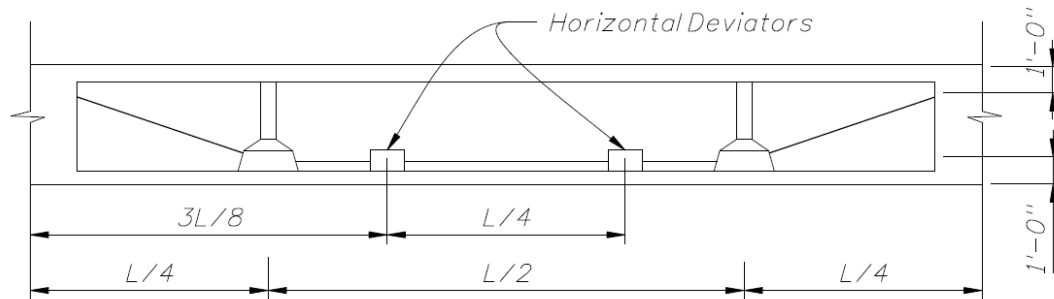
Figure 3 Typical Span Post-Tensioning Tendon Layout

MODELING

Three-dimensional Finite Element Method (FEM) is used to model the bridges. The box and diaphragms are modeled with 4-node shell elements with each node having 3 translational and 3 rotational degrees of freedom (DOFs). Prestressing tendons are combined into a single element located at the tendon centroid on either side of the box and modeled using truss elements with one DOF for each node. For simplicity, no losses are included in the effective prestress in the tendons. Self-weight load is modeled with body acceleration force. Post-tensioning force is achieved through equivalent thermal loading within the tendon elements, since proper temperature drop in tendon element will result in the same initial forces in tendons as in post-tensioning. Live load is modeled using nodal loads; for a single truck, six nodal loads are used at the wheel centers as described in AASHTO LRFD. Figure 4 shows the partial mesh of the finite element model of the 300 ft radius bridge, and the mesh at the post-tensioning tendon anchorage.
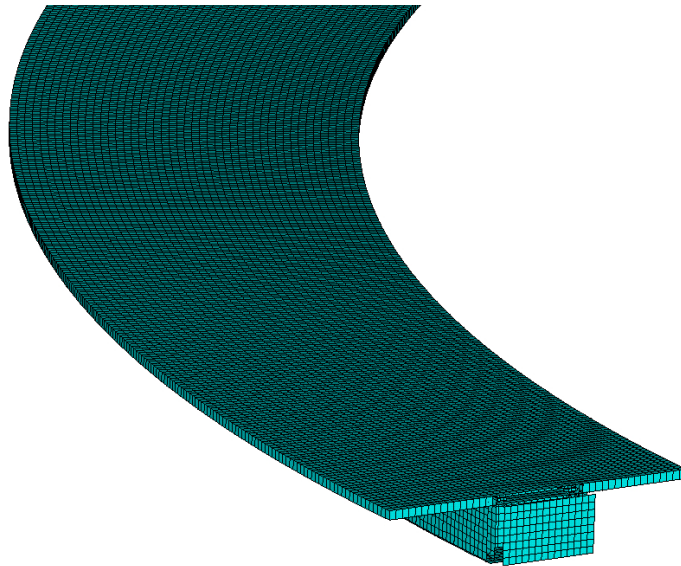
(a) Radius = 300ft
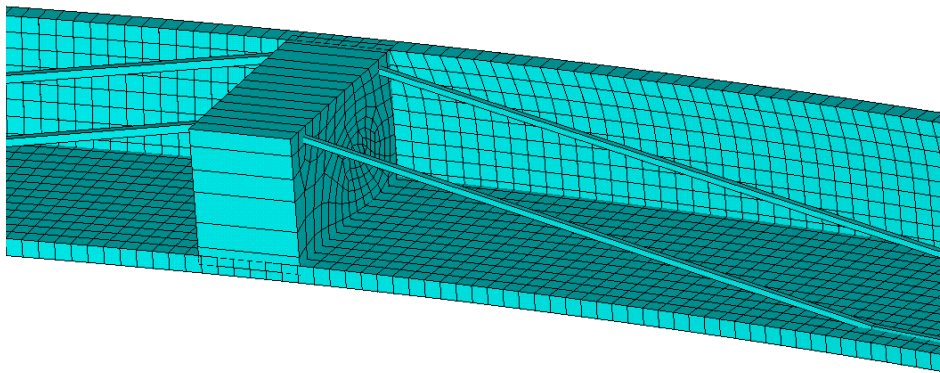

(b) Post-tensioning Anchorage Mesh

Figure 4 FEM Mesh

RESULTS

Curvature effects on normal stress, shear stress and bearing reactions due to the applied loads (self-weight, post-tensioning and combined effects) are investigated through both magnitude and ratios of these effects in curved bridges to corresponding straight bridges.

Neglecting time dependent effects, the combined results of self weight and post-tensioning may be regarded as the final service state.
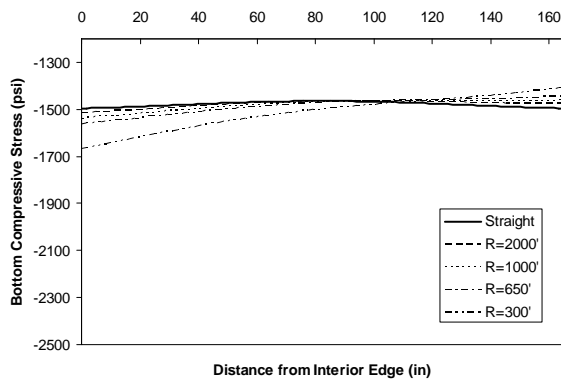
NORMAL STRESS

Since tensile stress at the positive moment zone is generally the controlling design criteria for post-tensioned bridges, the normal stress investigation is concentrated on the bottom tensile stresses at both end spans and center span. The sections under consideration include a section at 55' from the end support in the end spans, and a section at mid-span for center span. These are the maximum positive moment sections from the straight bridge model under self weight.
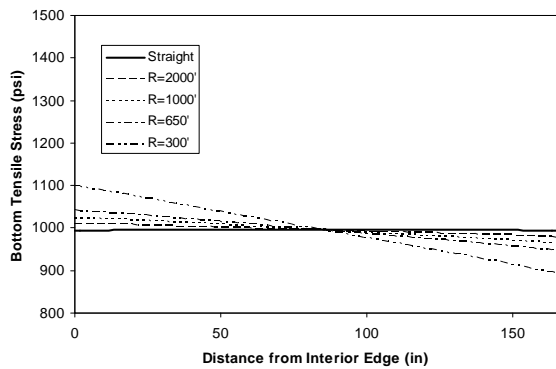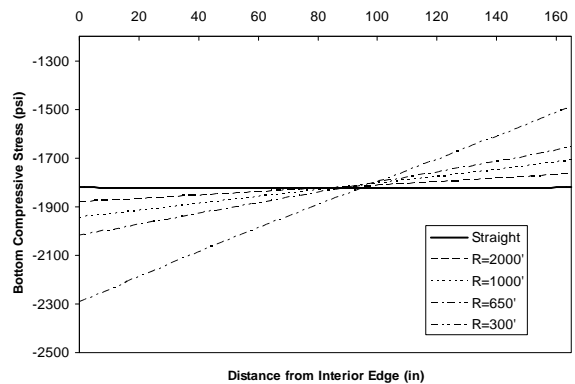

(a) End Span Section Bottom Tensile Stress Due to Self Weight
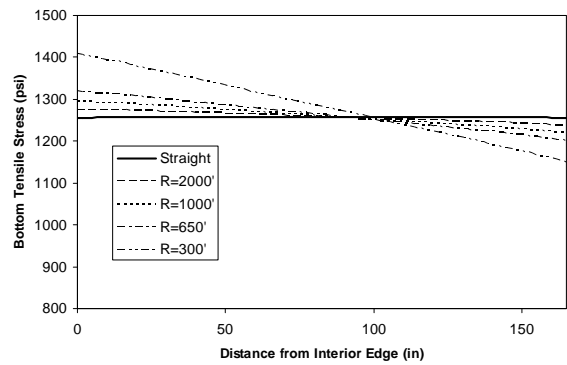
(b) Center Span Section Bottom Tensile Stress Due to Self Weight

(c) End Span Section Bottom Compressive Stress under Post-Tensioning

(d) Mid Span Section Bottom Compressive Stress under Post-Tensioning

Figure 5 Normal Stress Transverse Distribution at Different Locations

Figure 5 shows the normal stress distribution along the bottom slab and its variation with curvature under both self-weight and post-tensioning loads. The straight bridge model has a symmetrical normal stress distribution across bottom slab in both load cases, while

curved bridges have more tensile stress on the interior side than the exterior side under self weight. Also, the interior edges are subjected to higher level of compressive stress under post-tensioning. The interior edge is defined as the edge with the smaller radius of curvature. As curvature increases, this effect becomes more significant which agrees with the warping stress distribution for boxed sections due to curvature.

The ratios of the center span bottom normal stress for the curved bridges to those for the straight bridge are presented in Figure 6. Dead load and post-tensioning normal stresses do not vary significantly with curvature, while combined stress is sensitive to curvature. If a maximum normal stress ratio of 5% is used to determine whether a straight model is adequate to estimate the normal stress of curved ones, the central angle can reach 22 degrees and 11 degrees, for self weight post-tensioning load cases, respectively. However, for combined stress results, it is limited to 4 degrees. This effect can be explained by the canceling nature of normal stresses due to self weight and post-tensioning, and has to be determined on case-by-case basis.
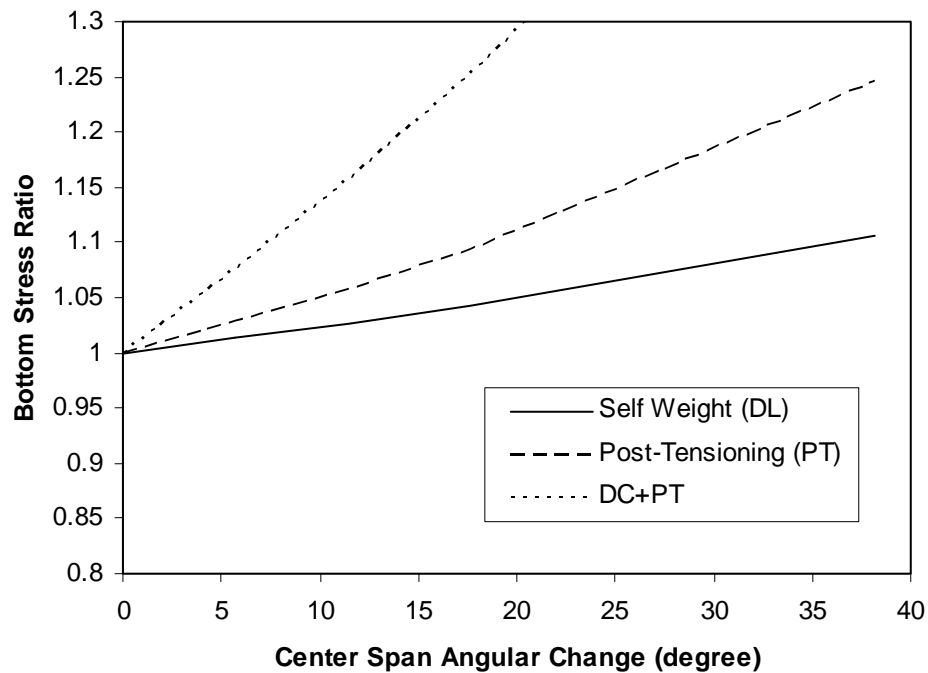

Figure 6 Center Span Section Bottom Stress Variation with Curvature

Live load effect on the bottom slab tensile stress is also investigated. Although AASHTO LRFD live load models include both lane load and truck/tandem load, only the HL-93 truck load is considered to study the normal stress distribution under concentrated live loads for curved bridges. Three transverse truck locations are included: interior edge, center line of the box section and exterior edge, with rear axle at the mid span section of the center span for all cases.

Figure 7 shows the bottom slab normal stress distribution under different truck locations and different curvatures. The curvature is represented by center span angles. Maximum stresses at interior edge and exterior edge are compared. It is observed that as the center span angle increases, the tensile stress at interior edge increases while the tensile stress at exterior edge decreases. The curvature effects are moderate. The maximum differences between curved bridges and the straight bridge are 14% and 10% among all the load cases for interior edge stress and exterior stress, respectively. Both maximum differences occur under loading on the side opposite the point of interest for the bridge with the largest span angle (not the most critical load cases). For the critical load cases, the differences are 7% and 4% for the interior edge and the exterior edge, respectively.
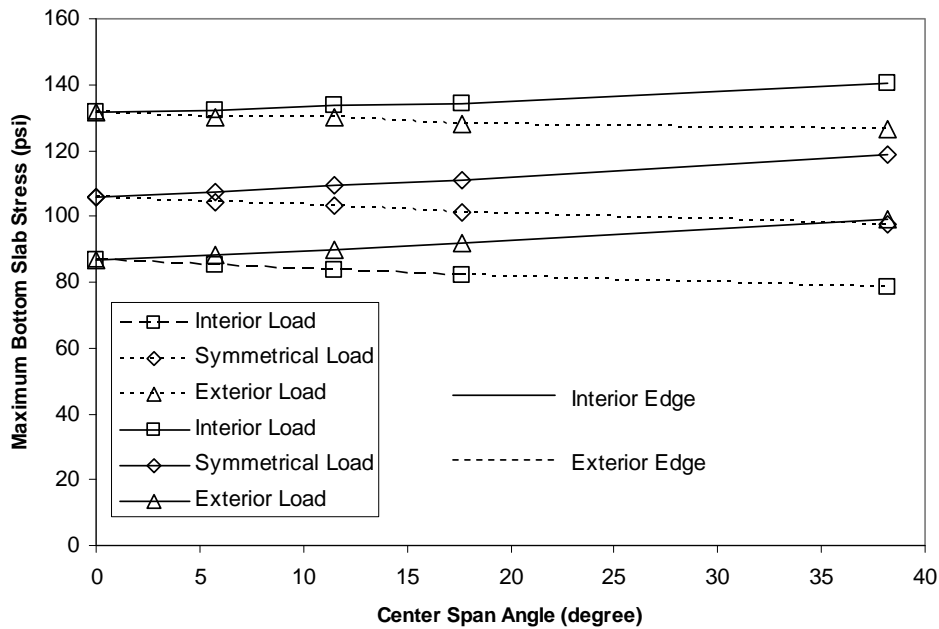

Figure 7 Maximum Bottom Slab Stress Due to HL-93 Truck

SHEAR STRESS

Shear stresses are compared along the vertical axis for both webs of the center span at sections 9 feet away from the intermediate piers. The section was chosen to minimize localized support and tendon anchoring effects while maintaining a section within the high shear force region. Figure 8 presents the shear stress distribution along the box depth for both interior and exterior webs, in which positive shear stresses are acting in the positive coordinate direction on the positive face.
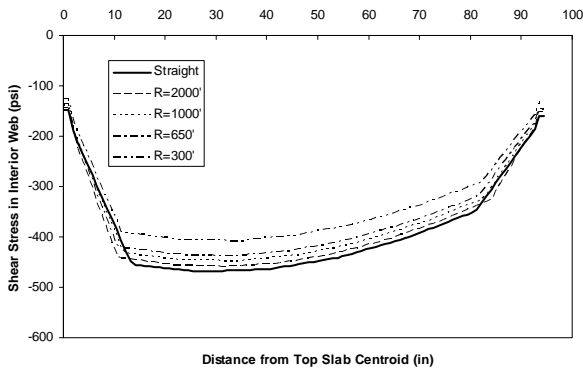
(a) Interior Web Shear Stress Due to Self Weight
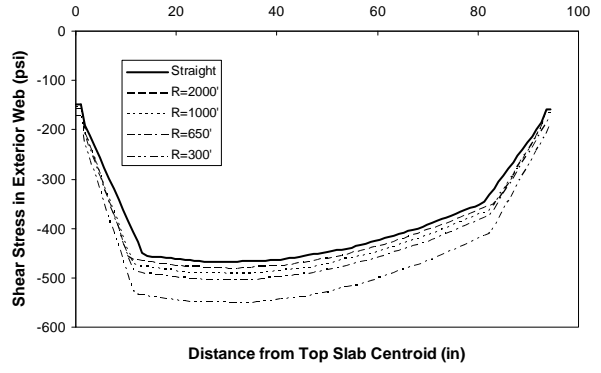
(b) Exterior Web Shear Stress Due to Self Weight
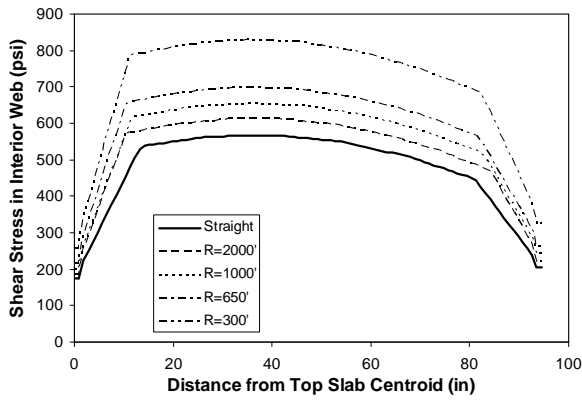
(c) Interior Web Shear Stress Due to Post-Tensioning

(d) Exterior Web Shear Stress Due to Post-Tensioning
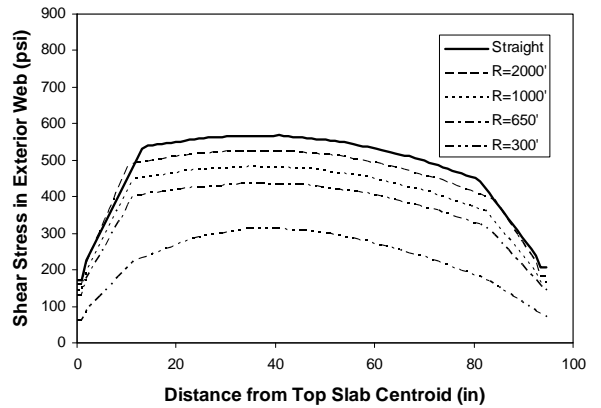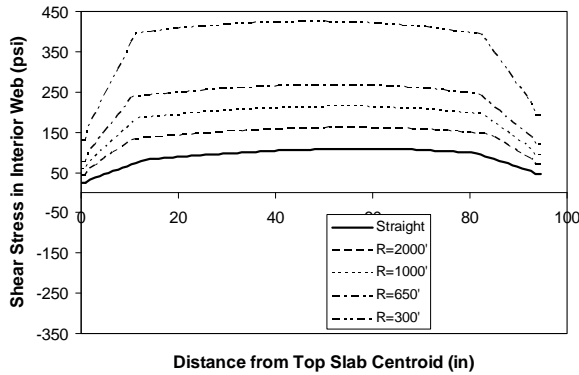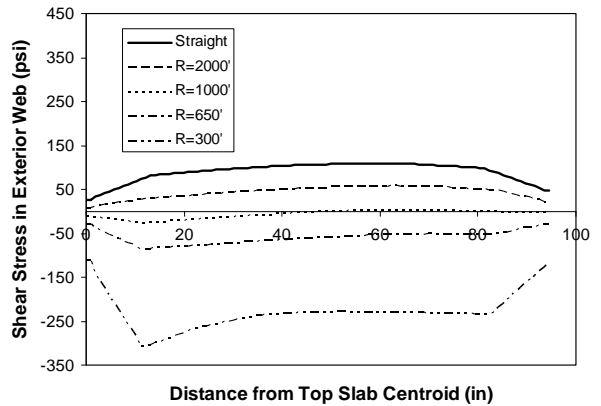

(e) Interior Web Shear Stress Due to Combined Effects

(f) Exterior Web Shear Stress Due to Combined Effects

Figure 8 Shear Stress Distribution along Webs

The shear stress distribution along webs under dead or post-tensioning load is as expected. Under self-weight, exterior webs take more shear stress than interior webs for curved bridges. As the curvature radius decreases, the exterior web shear stress increases while the interior web shear stress decreases. The difference is rather moderate. The maximum shear stresses in both webs for the straight bridge are -469 psi. For the 300-ft radius bridge, the maximum shear stresses are -407 and -551 psi for the interior and the exterior webs, respectively. This yields a 13% and 18% difference from the straight bridge results.

Under post-tensioning load, shear stress is opposite to that in the self-weight load case. Interior webs are subjected to more shear stress than exterior webs. As the curvature radius decreases, the difference becomes much more considerable than that under self-weight. For the 300-ft radius bridge, the maximum post-tensioning stresses are 829 and 313 psi in the interior and the exterior web, respectively. This is a 46% and 45% difference from straight bridge results.

For the combined load case, it is noted that shear stress levels have been reduced significantly from the self weight load case for the straight model; from 469 to 109 psi. However for the curved bridges due to two opposite shear stress distributions among interior and exterior webs under self weight and post-tensioning, as the curvature radius decreases, the results become less favorable in comparison to the straight model. For the 300-ft radius bridge, the combined shear stress in interior web is 425 psi, while the dead load shear stress is -407 psi. Although post-tensioning provides a magnitude of shear stress in the interior web twice that of the self-weight effect in the opposite direction, post tensioning will not help with reducing dead load shear stress. However, for exterior webs within moderate curvature range, post-tensioning can efficiently reduce dead load shear stresses.

BEARING REACTION

Torsional moment in box sections will cause uneven bearing reactions at piers and end bents when the loads are transferred to substructure. If not properly considered, unexpected bearing uplift is likely to happen. Although in practice there are ways to minimize this effect, two symmetrical supports are provided at each pier location to study this effect.

Both interior and exterior bearing reaction results under dead load, post-tensioning, and combined loads are presented in Table 2. The positive sign represents compressive bearing reactions, while the negative sign stands for bearing uplift. It is expected that the effects of torsional moment on the differing bearing reactions will be greater in curved bridges. Under dead load, exterior bearings will take more reaction than interior bearings. The bearing reaction ratios between exterior and interior bearings range from 1.00 to 3.31 at end pier locations and from 1.00 to 1.06 at intermediate pier locations. When post-tensioning the external tendons, bearing reactions due to post-tensioning are caused by secondary prestressing effects. For the straight bridge model, intermediate piers are subjected to uplifting forces while end piers take compressive forces. As curvature increases, exterior

bearings tend to take a more compressive reaction, while interior bearings are subjected to more uplifting reaction. For tight curvatures (300-ft radius), the end interior bearings start uplifting, while the intermediate interior bearings experience ten times more uplifting force than that of the straight bridge. The end exterior bearing reactions increase by two times, while intermediate exterior bearings experiences ten times the compressive reaction than that of the straight bridge. For the combined results of self-weight and post-tensioning, the net bearing reactions are compressive for all cases. It should be noted the curvature has significant effects on the bearing reactions. For very flat curvatures (2000 ft radius), the reaction difference between exterior bearing and interior bearing is about 30% to 40%, while for tight radii (300 ft radius), the exterior bearing virtually takes the total pier reaction.

Table 2 Bearing Reactions under Different Loading (in kips)

(a) End Pier Locations

	Self Weight (DL)		Post-Tensioning (PT)		DL + PT	
	Interior Bearing	Exterior Bearing	Interior Bearing	Exterior Bearing	Interior Bearing	Exterior Bearing
Infinite	412	412	115	115	527	527
2000	379	445	81	148	460	593
1000	345	478	47	181	392	659
650	309	514	10	215	319	728
300	190	629	-109	316	81	944

(b) Intermediate Pier Locations

	Self Weight (DL)		Post-Tensioning (PT)		DL + PT	
	Interior Bearing	Exterior Bearing	Interior Bearing	Exterior Bearing	Interior Bearing	Exterior Bearing
Infinite	1367	1367	-115	-115	1252	1252
2000	1355	1380	-300	71	1055	1451
1000	1346	1393	-485	257	861	1650
650	1339	1407	-678	453	661	1860
300	1354	1434	-1292	1085	61	2520

Figure 9 compares the bearing reaction ratios between curved and straight bridges for all the load cases. Although the bearing reaction should be discrete points in the charts, continuous curves connecting data points for each bridge are used to better show the changes. It can be observed that for dead load, the curvature has a much higher impact on the end pier bearings, while for post-tensioning forces, there is more impact on the intermediate pier bearings. However, under combined loads of self-weight and post-tensioning, this difference in curvature effects on end pier and intermediate pier bearing reactions gets mostly eliminated.

(a) Self Weight (DL)

(b) Post-Tensioning (PT)

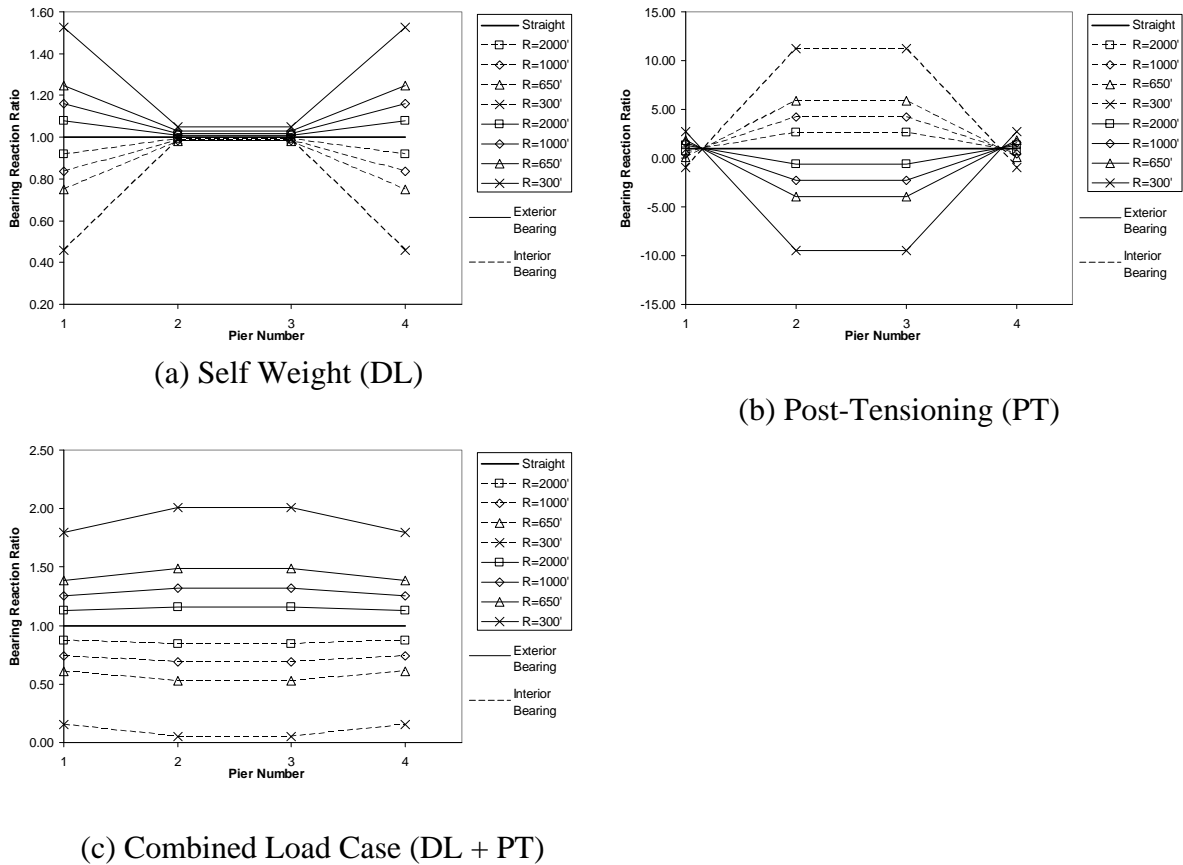
(c) Combined Load Case (DL + PT)

Figure 9 Bearing Reaction Ratios

It is also noted that although exterior or interior bearing reaction is significantly affected by curvature effects, the total reaction (sum of exterior and interior bearing reactions) at each pier location will only be slightly changed. The maximum variance of total pier reactions in curved bridges from straight model are 2%, 10%, and 3% when subjected to self-weight, post-tensioning and the combined load, respectively.

CONCLUSIONS

Curvature effects on concrete box-girder bridges are investigated by FEM analysis. Analytical results show that a simplified straight bridge model is not appropriate to directly estimate the important structural response for curved bridges. Utilizing 3D models or developing proper modification methods on a straight bridge model is crucial to obtain good design results for curved box-girder bridges with post-tensioning. The following conclusions can be drawn to benefit design practice.

(1) Normal stress due to individual self-weight or post-tensioning load does not vary significantly as curvature changes. A central angle up to 15 degrees can result in a 5% difference in normal stress between curved and straight bridges for either load case. However, for combined load effects, due to the opposition of these two load effects, the results vary significantly as curvature increases. A central angle of 15 degree can cause 20%, 124% and 42% differences in the combined normal stress, shear stress and bearing reactions, respectively.

(2) Using post-tensioning to reduce shear stress levels in concrete is not as effective in curved bridges in comparison to straight bridges. The reason is not the increase of dead load torsion effect due to curvature, but the unfavorable post-tensioning shear stress distribution among webs. Efforts of trying to reduce concrete shear stress levels by merely increasing post-tensioning tendon quantity will not work effectively for sharply curved bridges. Other methods need to be explored to meet the shear design criteria, if required.

(3) Among all the three structural responses investigated in this study, bearing reaction is the most sensitive structural response to curvature. With very flat curvatures (Radius = 2000 ft), the bearing reaction can be 30% to 40% different from that in straight bridge. For tight curvature bridges, under self-weight and post-tensioning only, one bearing virtually takes the total pier reaction.

It should be noted that compared to internal tendons, external post-tensioning tendons in curved bridges have a horizontal eccentricity towards the interior edge except for at deviator locations, as they are normally placed in symmetry across the section. The validity of the conclusions from this study needs to be verified for internally prestressed structures and bridges with different boundary conditions, construction methods, and structural systems.

ACKNOWLEDGEMENT

REFERENCES

1. AASHTO (2007). "LRFD Bridge Design Specifications - 4th Edition." American Association of State Highway and Transportation Officials, Washington, DC

2. Eduardo A.B. Salse. (1971). "Analysis and Design of Prestressed Concrete Circular Bow Girders for Bridge Structures." American Concrete Institute, Special Publication, Vol.26, pp 714-740.

3. Thompson, M.K. at al. (1998). "Measured Behavior of a Curved Precast Segmental Concrete Bridge Erected by Balanced Cantilevering.", Research Report 1404-2, Center for Transportation Research, University of Texas, Austin, TX

4. Tung. D. H. H., and R. S. Fountain.(1970). "Approximate Torsional Analysis of Curved Box Girders by the M/R-Method," Engineering Journal, American Institute of Steel Construction. Vol. 7, No.3, pp. 65-74.

5. United States Steel. (1984). "V-Load Analysis;' Available from the National Steel Bridge Alliance, Chicago, IL. pp. 1-56.

6. Magdy Samaan, Khaled Sennah, and John B. Kennedy. (2002) "Positioning of bearings for curved continuous spread-box girder bridges." Can. J. Civ. Eng. 29(5): 641–652